Scaling laws for impact fragmentation of spherical solids

G. Timár,[1] F. Kun,[1,*] H. A. Carmona,[2] and H. J. Herrmann[3,4]
[1]*Department of Theoretical Physics, University of Debrecen, P. O. Box 5, H-4010 Debrecen, Hungary*
[2]*Centro de Ciências e Tecnologia, Universidade Estadual do Ceará, 60740-903 Fortaleza, Ceará, Brazil*
[3]*Departamento de Física, Universidade Federal do Ceará, 60451-970 Fortaleza, Ceará, Brazil*
[4]*Computational Physics IfB, HIF, ETH, Hönggerberg, S-8093 Zürich, Switzerland*
(Received 16 May 2012; published 27 July 2012)

We investigate the impact fragmentation of spherical solid bodies made of heterogeneous brittle materials by means of a discrete element model. Computer simulations are carried out for four different system sizes varying the impact velocity in a broad range. We perform a finite size scaling analysis to determine the critical exponents of the damage-fragmentation phase transition and deduce scaling relations in terms of radius R and impact velocity v_0. The scaling analysis demonstrates that the exponent of the power law distributed fragment mass does not depend on the impact velocity; the apparent change of the exponent predicted by recent simulations can be attributed to the shifting cutoff and to the existence of unbreakable discrete units. Our calculations reveal that the characteristic time scale of the breakup process has a power law dependence on the impact speed and on the distance from the critical speed in the damaged and fragmented states, respectively. The total amount of damage is found to have a similar behavior, which is substantially different from the logarithmic dependence on the impact velocity observed in two dimensions.

DOI: 10.1103/PhysRevE.86.016113 PACS number(s): 46.50.+a, 45.05.+x, 05.10.−a, 62.20.M−

I. INTRODUCTION

Fragmentation (i.e., the sudden disintegration of solids into smaller pieces) is a ubiquitous process that underlies many natural phenomena and industrial processes [1]. Energetic loading giving rise to the breakup of solids is typically exerted by projectile shooting, explosion, or impact with a hard wall. Recently, the impact fragmentation of materials has attracted intensive research since it forms the basis of comminution, crushing, milling, and grain liberation in industrial processes. Driven by the scientific importance and industrial needs, the intensive research of the last two decades revealed that the mass distribution of fragments showed a power law behavior with universal exponents. The value of the exponent was mainly determined by the effective dimensionality of the system [2–5] and by material behavior such as brittleness and plasticity [6].

Due to the complexity of the breakup process, theoretical studies were usually based on computer simulations of discrete element models (DEM) of disordered materials [7,8]. In the framework of DEM, the sample was represented as an assembly of cohesive elements making possible a realistic treatment of materials' microstructure and of the loading conditions. Computer simulations of such models proved to reproduce the experimental findings and revealed the underlying mechanism of the emergence of universal power laws: increasing the imparted energy a phase transition took place from the damaged to the fragmented state, which proved to be of the second order [9].

In spite of the large amount of experimental and theoretical efforts of the last decades, several questions remained open on fragmentation phenomena. Although the damage-fragmentation transition has been confirmed experimentally [10–12], very little is known about the critical exponents and about the effect of dimensionality on the phase transition. Recent computer simulations of a generic model of impact fragmentation of solids led to the surprising result that the exponent of the mass distribution is not universal. It was shown that a power law distribution appeared at the transition point, however, the exponent increased with increasing impact velocity in the fragmented regime [13,14]. The result questioned the universality and the validity of the phase transition nature of fragmentation phenomena.

To settle these problems, in the present paper, we investigate the fragmentation of spherical bodies due to impact with a hard wall focusing on the transition from the damaged to the fragmented state. We carry out computer simulations at four different system sizes varying the impact velocity within a broad range. Based on finite size scaling analysis of the mass of the largest fragment and of the average fragment mass, we determine the critical exponents of the damage-fragmentation transition with good accuracy. Our calculations reveal that the exponent of mass distribution does not depend on the impact velocity (i.e., the apparent increase of the exponent can be removed by taking into account that the cutoff mass diverges when approaching the critical point from above). Starting from the scaling analysis of the rate of damaging we derive the dependence of the total damage on the impact velocity: In spite of the logarithmic dependence predicted by DEM simulations in two dimensions, very interestingly we find a power law behavior in three dimensions. The characteristic time scale of the breakup process is found to decrease as a power law of the impact velocity similarly to the behavior of the duration of Hertz-type contacts. However, in the fragmented regime a power law is obtained as a function of the distance from the critical point. Besides their theoretical importance, the scaling relations can also be exploited in engineering design.

II. DISCRETE ELEMENT MODEL OF IMPACT

We carry out molecular dynamics simulations of the impact of a spherical solid body with a hard wall using a DEM of

*ferenc.kun@science.unideb.hu

heterogeneous brittle materials in three dimensions. The model was introduced by the authors of Ref. [15] as an extension of two-dimensional DEMs using beam elements. In the model, the spherical sample is represented as a random packing of spheres with a bimodal distribution. The particles interact via the Hertz contact law when they are pressed against each other. Cohesive interaction is provided by beams which connect the particles along the edges of a Delaunay triangulation of the initial particle positions. In three dimensions the total deformation of a beam is calculated by the superposition of elongation, torsion, as well as bending and shearing in two different planes [15]. The effect of the hard wall during the impact process is captured in such a way that for those particles which overlap with the wall a restoring force is introduced proportional to the overlap distance. The time evolution of the system is determined by molecular dynamics simulations solving the equation of motion of the spherical particles [15–17]. During the simulations, the beams break when they get overstressed according to a physical breaking criterion [7,8,15]

$$\left(\frac{\varepsilon}{\varepsilon_{th}}\right)^2 + \frac{\max(|\theta_i|,|\theta_j|)}{\theta_{th}} \geqslant 1, \qquad (1)$$

where ε denotes the longitudinal strain, furthermore, Θ_i and Θ_j are the generalized bending angles at the two beam ends. The two terms of Eq. (1) characterize the contribution of the stretching and bending failure modes of a beam: The increase of a threshold value decreases the importance of the corresponding breaking mode. The parameters of the model were set in Ref. [15] after carefully testing the cracking mechanisms of spherical solid bodies. In our simulations both breaking thresholds were set to constant values $\varepsilon_{\rm th} = 0.03$ and $\Theta_{\rm th} = 3$ degrees which implies that only structural disorder is present in the sample.

We carried out computer simulations of the impact process varying the initial velocity v_0 in a broad range for four different system sizes R. To keep the problem numerically tractable, we considered samples of fixed radius $R = 3.5, 5.63, 7.03, 8.12$ mm where the average radius of single particles is $\bar{r} = 0.5$ mm. The particle number fluctuates in the samples around the average values $\langle N\rangle = 1763, 7337, 14\,285, 22\,013$. In the simulations the time evolution of the system is stopped when there is no beam breaking during 1000 time steps. Fragments are identified in the final state as sets of particles connected by the surviving beams. Further details of the model construction together with the parameter settings and test simulations can be found in Ref. [15].

For impact fragmentation of spheres it has been shown in Ref. [15] that our DEM reproduces the experimentally observed dynamics of crack formation and breakup scenarios to a good accuracy. In the present paper we focus on the transition from the damaged to the fragmented state in impact-induced breakup as the impact velocity is gradually increased. In the limit of very low impact velocities no beam breaking occurs (i.e., the sample gets deformed and rebounds from the wall without any damage). Simulations have shown that in this case the impact process can be described by the Hertz theory [18,19]. The main characteristic quantities of the Hertz impact obey simple power law scaling with the impact velocity. The behavior of the maximum deformation $h \sim v_0^{4/5}$ and of the duration of contact $\tau \sim v_0^{-1/5}$ is reproduced by our DEM simulations with a good precision.

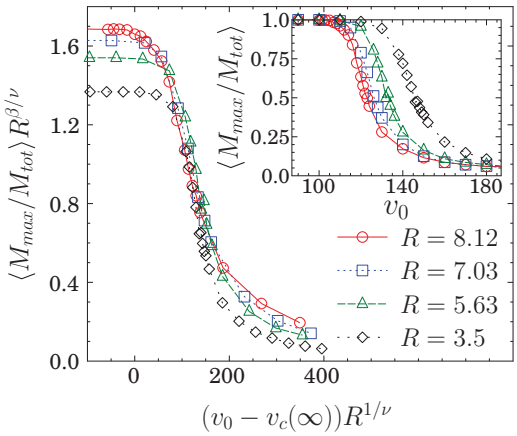

FIG. 1. (Color online) Inset: Mass of the largest fragment normalized by the total mass of the sample $\langle M_{\rm max}/M_{\rm tot}\rangle$ as a function of the impact velocity v_0 for different system sizes. Main panel: Scaling collapse obtained by rescaling the two axes according to Eq. (4).

III. DAMAGE-FRAGMENTATION TRANSITION

Increasing the impact velocity the sample gets damaged and gradually breaks into pieces. The degree of breakup can be quantitatively characterized by the mass of the largest fragment $M_{\rm max}$ compared to the total mass of the body $M_{\rm tot}$ [9,20]. Simulations reveal that, depending on the impact velocity, the final outcomes of the breakup process of the spherical sample fall into two substantially different classes: At low impact velocities some cracks appear, however, the sample retains its integrity. Broken bonds form cracks which initiate from the contact surface with the hard wall, however, they get arrested without creating fragments or only some very small pieces are chopped out of the sample. Cracks are concentrated inside a conical volume (Hertz cone [18,19]), whose base is the contact circle with the hard wall. Consequently, in the final state of the process only small fragments comprising only a few spheres can be observed [15]. This low velocity regime is the damage phase of the system, where the mass of the largest fragment is practically equal to the total mass of the sample $M_{\rm max}/M_{\rm tot} \approx 1$. To achieve complete breakup the impact velocity has to exceed a threshold value v_c above which even the largest fragment becomes significantly smaller than the original body $M_{\rm max}/M_{\rm tot} \ll 1$. This first happens when meridional cracks starting from the Hertz cone reach the surface of the sample opposite to the impact site [15]. Further increasing v_0, segmentation cracks are formed between meridional cracks further reducing the size of fragments [15]. The inset of Fig. 1 presents the sample average of the fraction of the largest fragment $\langle M_{\rm max}/M_{\rm tot}\rangle$ as a function of the impact velocity for the four different system sizes R considered. [The scaling exponents used in the main panel of the figure are those extracted later in Eqs. (3) and (4).] It can be observed that the curves are monotonically decreasing and exhibit a curvature

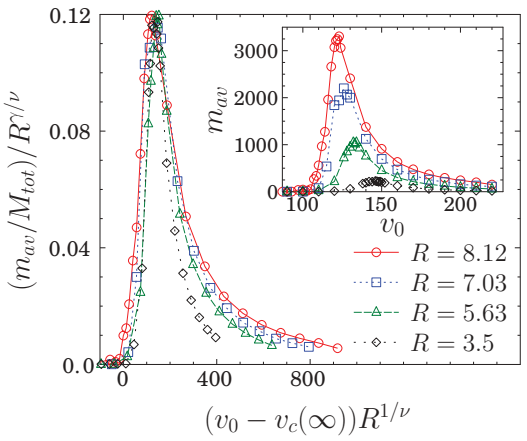

FIG. 2. (Color online) Inset: Average fragment mass as a function of the impact velocity for different system sizes. Main panel: Rescaling $m_{\rm av}$ and the impact velocity v_0 by an appropriate power of R, the curves corresponding to different system sizes collapse on a master curve.

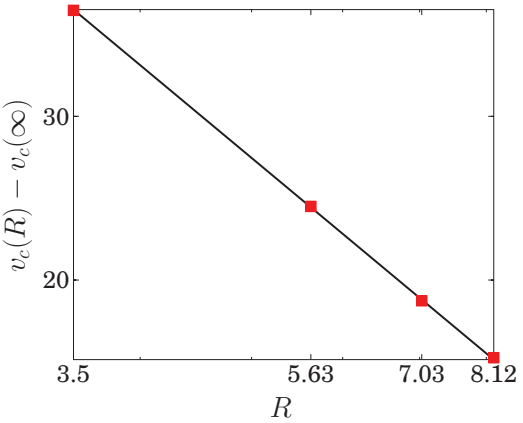

FIG. 3. (Color online) Difference between the critical value of the impact velocity of finite and infinite systems $v_c(R) - v_c(\infty)$ as a function of the system size R. The value of $v_c(\infty)$ was tuned to obtain the best quality power law according to Eq. (3).

change at $v_c(R)$, which can be identified as the transition point from the damaged to the fragmented regime [9,20]. Note that with increasing system size R the transition gets sharper and the transition point shifts to lower values as typically observed for continuous phase transitions. It has been shown by the authors of Ref. [9] that the strength of the largest fragment $\langle M_{\rm max}/M_{\rm tot}\rangle$ can be considered to be the order parameter of the transition.

The damage-fragmentation transition becomes more transparent by investigating the average fragment mass $m_{\rm av}$. It is defined as the sample average (denoted by $\langle\cdot\rangle$) of the ratio of the second M_2 and first M_1 moments of fragment masses

$$m_{\rm av} = \langle M_2/M_1\rangle. \tag{2}$$

Here the kth moment M_k of the fragment mass distribution is defined in a single fragmentation event of n fragments with masses m_i $(i = 1,\ldots,n)$ as $M_k = \sum_{i=1}^{n} m_i^k - M_{\rm max}^k$. Note that the contribution of the largest fragment of mass $M_{\rm max}$ is subtracted from M_k. Finally, $m_{\rm av}$ is obtained by averaging the ratio M_2/M_1 over a large number of simulations [9,21,22]. It can be observed in the inset of Fig. 2 that $m_{\rm av}$ has a peak which gets sharper with increasing R. [The scaling exponents used in the main panel of the figure are those extracted later in Eqs. (3) and (5).] We determined the finite size dependent effective critical point $v_c(R)$ of the system as the position of the maximum of $m_{\rm av}$ which coincides with the point of curvature change of $\langle M_{\rm max}/M_{\rm tot}\rangle$ with a reasonable precision. The critical velocities are $v_c(R_1) = 146$ m/s, $v_c(R_2) = 131$ m/s, $v_c(R_3) = 126$ m/s, and $v_c(R_4) = 123.5$ m/s. Assuming the scaling form for the critical velocity

$$v_c(R) = v_c(\infty) + AR^{-1/\nu}, \tag{3}$$

in terms of the system size [21,22] we determined the critical velocity of the infinite system $v_c(\infty)$ and the correlation length exponent ν of the transition. In Fig. 3 a power law is obtained with an excellent quality by setting $v_c(\infty) = 107$ m/s in Eq. (3).

The value of the exponent ν was obtained by fitting $\nu = 1.00 \pm 0.05$. The result implies that in the limit of very large system sizes the critical velocity of the damage-fragmentation transition converges to $v_c(\infty)$. Starting from the finite size scaling of the critical velocity Eq. (3) we can analyze the size dependence of the normalized mass of the largest fragment. Since $\langle M_{\rm max}/M_{\rm tot}\rangle$ is the order parameter of the damage-fragmentation transition, it is reasonable to assume the scaling

$$\left\langle \frac{M_{\rm max}}{M_{\rm tot}} \right\rangle (v_0, R) = R^{-\beta/\nu} F^{(1)}\{[v_0 - v_c(\infty)]R^{1/\nu}\}, \tag{4}$$

where β is the order parameter critical exponent and $F^{(1)}$ denotes the scaling function. It can be observed in Fig. 1 that rescaling the impact velocity v_0 and $\langle M_{\rm max}/M_{\rm tot}\rangle$ according to Eq. (4) the curves obtained at different system sizes can be collapsed with reasonable accuracy. In Fig. 1 only the value of β is tuned providing $\beta = 0.25 \pm 0.03$, while for ν and $v_c(\infty)$ the above values were inserted. It can also be seen in the figure that the data collapse has the best quality in the vicinity of the transition point as it is expected.

The average fragment mass with the above definition characterizes the fluctuations of fragment masses [9,21], hence, the finite size scaling analysis of $m_{\rm av}$ reveals the γ exponent of the damage-fragmentation transition. Assuming that the system has a continuous phase transition, the scaling

$$m_{\rm av} = R^{\gamma/\nu} F^{(2)}\{[v_0 - v_c(\infty)]R^{1/\nu}\}, \tag{5}$$

should hold [21,22], where $F^{(2)}$ denotes the scaling function. Figure 2 illustrates the good quality data collapse of the $m_{\rm av}$ curves, which was obtained by inserting the above value of ν and $v_c(\infty)$ varying γ as the only free parameter of the functional form Eq. (5). The best collapse was obtained with the exponent $\gamma = 0.10 \pm 0.02$. For consistency, we also checked for the largest system size the validity of the behavior $m_{\rm av} \sim |v_0 - v_c(R)|^{-\gamma}$, which was fulfilled with the same γ within the error bars. It has to be emphasized that, strictly speaking, the finite size scaling laws hold in the limit of large system sizes. In Figs. 1 and 2 we intensionally keep the curves

of the smallest system $R = 3.5$ to show that with increasing system size R the quality of collapse rapidly improves.

IV. FRAGMENT MASS DISTRIBUTION

The most important characteristic quantity of the fragmenting system is the mass distribution of fragments $p(m)$. It has been shown in experiments that $p(m)$ exhibits a power law behavior

$$p(m) \sim m^{-\tau} \tag{6}$$

for small masses $m \ll M_{\text{tot}}$ at and above the critical point v_c [5,10,23–26]. The most striking observation on fragmentation phenomena is the universality of the exponent τ of the mass distribution: Fragmentation experiments on a large variety of heterogeneous materials have shown that the value of τ does not depend on materials' microstructure, on the way the energy is imparted, and on the relevant length scale [10,27–30]. It is mainly determined by the dimensionality of the system [2,4,9] and by the mechanical response (brittle or ductile) of the sample [6]. DEM simulations of fragmentation processes have been able to reproduce the power law functional form [2–6,15] with various types of cohesive interactions from Lennard-Jones solids [14,31–33] through spring lattices [30,33] to beam networks [4,8,15]. The concept of universality motivated the development of stochastic models of fragmentation [34,35], among which the crack branching-merging scenario proved to be very successful [36,37]. Recent DEM simulations of a generic model of brittle solids have reported a surprising result: The fragment mass exponent τ of a two-dimensional disk impacted against a hard wall was found to slowly increase with the imparted energy E_0. Based on the numerical analysis of the simulation data a logarithmic functional form was deduced $\tau \sim \ln E_0$ above the critical point [13,14].

The universality of the mass distribution exponent τ is a crucial problem not solely from the theoretical point of view, but it is also of practical importance in engineering design (e.g., when estimating the energy consumption or loading conditions in ore processing to achieve a desired size reduction). To settle the problem, we performed a large number of simulations for impact velocities above v_c and carried out a scaling analysis of the mass distributions $p(m)$ for our largest system. In Ref. [15] it has been shown that for impact velocities slightly above v_c the fragment mass distribution of impacting spheres is composed of two parts: For small fragment masses a power law distribution is obtained with an exponential cutoff

$$p(m) \sim m^{-\tau} e^{-m/m_0}, \tag{7}$$

while for the large ones $p(m)$ has a maximum which can be fitted with a Weibull or log-normal form. Here m_0 denotes the characteristic fragment mass. These outcomes are in agreement with the generic functional form proposed by the authors of Ref. [4] based on the stochastic nucleation of the first major cracks and the branching-merging scenario of the smaller ones. We selected impact velocities above v_c where the disturbing effect of the surviving large pieces can be avoided. The inset of Fig. 4 presents mass distributions at three different impact velocities. It can be observed that they can qualitatively be described by the functional form of Eq. (7). Note that as the impact velocity v_0 approaches v_c from above the cutoff of the distributions moves towards larger values. To check whether the exponent τ of the distribution depends on v_0, we calculated the average fragment mass Eq. (2) and rescaled $p(m)$ with some powers of m_{av} along both axes. Figure 4 demonstrates that a high quality data collapse can be obtained with the scaling exponents $\kappa = 1.15 \pm 0.02$ and $\delta = 2.15 \pm 0.02$. The collapse implies that $p(m, v_0) m_{\text{av}}^{\delta}$ is only the function of m/m_{av}^{κ}, consequently the fragment mass distributions $p(m, v_0)$ obtained at different impact velocities v_0 must follow the scaling law

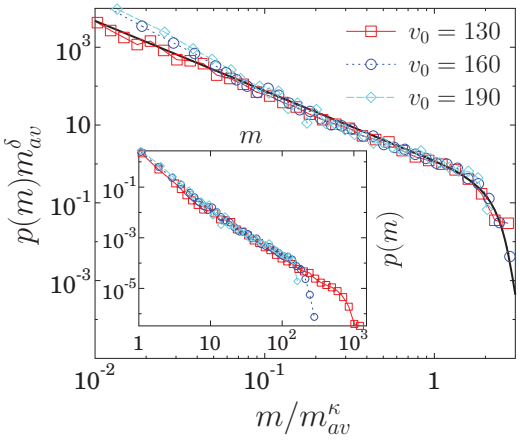

FIG. 4. (Color online) Inset: Mass distribution of fragments at different impact velocities for the largest system considered. Main panel: Rescaling the two axes with appropriate powers of the average fragment mass a high quality data collapse is obtained.

$$p(m, v_0) = m_{\text{av}}^{-\delta} \Phi\left(m/m_{\text{av}}^{\kappa}\right). \tag{8}$$

Here the dependence on the impact velocity v_0 is contained in m_{av}. Since $\kappa \approx 1$, the scaling function Φ in Eq. (8) is consistent with Eq. (7), widely used in the literature. In Fig. 4 the bold black line is fitted to the scaling function using Eq. (7) from which the value of τ can be determined accurately as $\tau = 1.8 \pm 0.05$. Deviations from the scaling function occur solely in the regime of small fragment masses due to the existence of unbreakable units (discrete elements) of DEM. It follows from the condition of normalization of the distributions that the three exponents τ, δ, and κ must fulfill the relation

$$\delta = \tau\kappa. \tag{9}$$

Substituting the numerical values, it can be seen that relation Eq. (9) holds with a good precision. We note that the scaling law Eq. (8) in terms of the average fragment mass is expected to hold not only in the vicinity of the critical point, but also inside the fragmented regime since it only assumes the homogeneity of the mass distribution function [21].

It has to be emphasized that looking at the unscaled distributions in the main panel of Fig. 4 one may guess a spurious increase of the exponent of the power law regime. Our results demonstrate that this occurs due to the decrease of the cutoff of the distributions with increasing impact velocity, which can be removed by appropriate rescaling. Power law exponents should be numerically extracted by fitting the scaling function together with the cutoff. The importance of this careful evaluation of data has been demonstrated in other

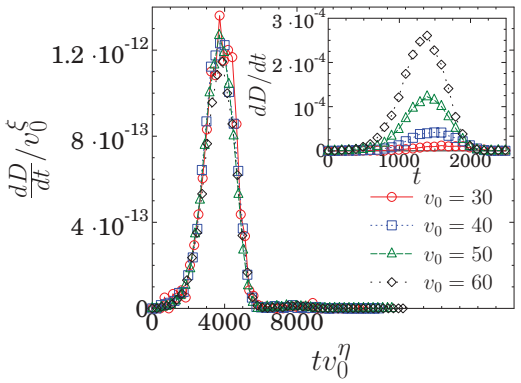

FIG. 5. (Color online) Time evolution of the breaking rate dD/dt for different values of the impact velocity below v_c. Rescaling the two axes with appropriate powers of v_0 excellent data collapse is obtained. The inset presents the original curves before rescaling.

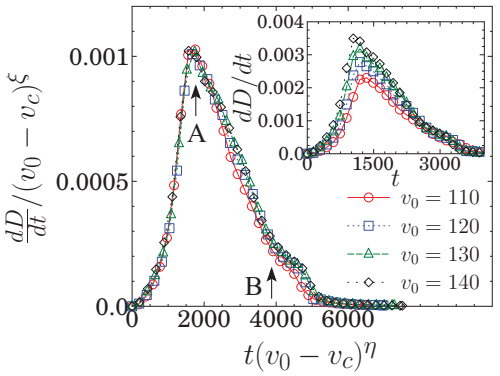

FIG. 6. (Color online) Time evolution of the breaking rate dD/dt for different impact velocities above v_c. High quality data collapse can be obtained by rescaling the two axes with powers of $v_0 - v_c$. The peak A and the inflexion point B of dD/dt mark the configurations where unloading sets in, and the sample rebounds from the wall, respectively. The inset presents the original curves before rescaling.

fields of physics as well, both for experiments [38,39] and for computer simulations [40].

V. TIME EVOLUTION OF DAMAGE

The above analysis of the phase transition of fragmentation required the investigation of the final state of the breakup process. On the microlevel, cracks are generated by breaking beams such that fragments form when cracks either completely surround a set of particles connected by surviving beams, or cracks span from surface to surface of the body. The total amount of broken beams and their spatial arrangement (i.e., crack structure) strongly depend on the impact velocity. The cracking mechanism leading to the formation of meridional and segmentation cracks of spherical bodies has been analyzed in detail in Ref. [15]. Now we focus on the time evolution of damage which is quantified by the fraction of beams $D(t) = N_b(t)/N$ that have been broken up to time t. Here $N_b(t)$ denotes the number of broken beams at time t and N is the total number of beams in the sample. Of course, $D(t)$ is a monotonically increasing function $[0 \leqslant D(t) \leqslant 1]$ whose derivative dD/dt provides the rate of beam breaking characterizing the breaking activity during the fragmentation process.

Breaking rate functions dD/dt are presented in the inset of Fig. 5 for the largest system size $R_4 = 8.12$ mm at four different impact velocities v_0 in the damage phase $v_0 < v_c$. It can be observed in the figure that the increase of the impact velocity v_0 has a dramatic effect on the damage rate: dD/dt has a maximum which becomes sharper and its position t_m shifts towards lower times with increasing v_0. Simulations showed that at the peak time t_m the deformation of the contact zone of the sphere with the hard wall reaches its maximum. It is important to emphasize that the breaking rate obtained at different impact velocities can be collapsed on a master curve by rescaling the two axes with some powers of v_0. In Fig. 5 a high quality data collapse is obtained with the exponents $\xi_d = 4.7 \pm 0.2$ and $\eta_d = 0.25 \pm 0.05$. The result implies that dD/dt follows the scaling law

$$\frac{dD(t,v_0)}{dt} = v_0^{\xi}\Psi\left(tv_0^{\eta}\right), \tag{10}$$

where Ψ denotes the scaling function.

Above the critical point $v_0 > v_c$ in the fragmented phase, the damage rate reaches much higher values (i.e., it can be observed in the inset of Fig. 6 that the functional form of dD/dt is qualitatively the same as in the damage phase, however, with an order of magnitude larger values than in Fig. 5). Simulations revealed that the peak time t_m is the point at which the compressive regime of the collision ends and unloading of the contact sets in. Along the decreasing branch of dD/dt an inflexion point emerges at the time when all fragments rebound from the hard wall (see Fig. 6). It is shown in Fig. 6 that the breaking rate functions obtained at different impact velocities can be again collapsed on a master curve by a rescaling transformation. A careful analysis of the simulated data shows that the scaling structure of dD/dt is the same Eq. (10) as in the damage phase, however, when replacing the impact velocity v_0 by the distance from the critical point $v_0 - v_c$. The scaling exponents providing the best collapse in Fig. 6 were determined numerically as $\xi_f = 0.33 \pm 0.05$ and $\eta_f = 0.11 \pm 0.02$.

A very important outcome of our scaling analysis is that the fragmentation process gets faster with increasing v_0, that is, the characteristic time scale t_c of the process follows

$$t_c \sim v_0^{-\eta_d}, \quad \text{for } v_0 < v_c, \tag{11}$$

$$t_c \sim (v_0 - v_c)^{-\eta_f}, \quad \text{for } v_0 > v_c. \tag{12}$$

It is interesting to note that the functional form of Eqs. (11) and (12) is similar to the behavior of the contact time of the elastic collision of spherical bodies with a hard plate [18,19]. In the damage phase η_d falls close to the exponent of Hertz contacts $\eta_d \approx \eta_h = 0.2$, however, in the fragmented regime the strong energy dissipation gives rise to a slower decrease of t_c characterized by a lower exponent $\eta_f < \eta_h$.

The total amount of damage D_{tot} accumulated until the end of the fragmentation process can be obtained by integrating the damage rate $dD/dt(t,v_0)$ over time from 0 to infinity

$$D_{\text{tot}}(v_0) = \int_0^{\infty} \frac{dD}{dt}(t,v_0)dt. \tag{13}$$

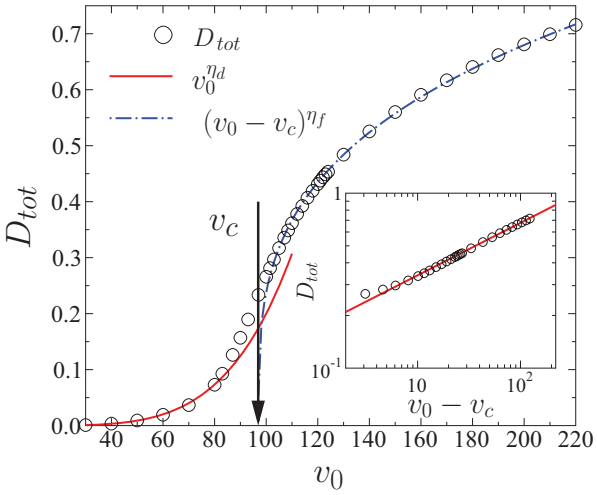

FIG. 7. (Color online) The total amount of damage $D_{\rm tot}$ as a function of the impact velocity. The red (continuous) and blue (dotted-dashed) lines correspond to the scaling laws Eqs. (11) and (12) of the damage and fragmented states, respectively. The vertical arrow indicates the critical impact velocity v_c. Inset: $D_{\rm tot}$ as a function of $v_0 - v_c$, where $v_c = 98$ was used. A good quality power law behavior is obtained. The slope of the straight line is $\eta_f = 0.29$.

Substituting the scaling form Eq. (10) it follows

$$D_{\rm tot}(v_0) = v_0^{\xi} \int_0^{\infty} \Psi\left(v_0^{\eta} t\right) dt, \tag{14}$$

where the integral can be performed by substituting t by $x = v_0^{\eta} t$. The calculations yield that the total amount of damage $D_{\rm tot}$ has a power law dependence on v_0 in the damage phase

$$D_{\rm tot} \sim v_0^{\alpha}, \tag{15}$$

while in the fragmentation phase a critical behavior is obtained

$$D_{\rm tot} \sim (v_0 - v_c)^{\alpha}. \tag{16}$$

The critical exponent α of the total damage is determined by the two scaling exponents of the damage rate

$$\alpha = \xi - \eta, \tag{17}$$

which have different values $\alpha_d = \xi_d - \eta_d = 4.45$ and $\alpha_f = \xi_f - \eta_f = 0.22$ in the damage and fragmented states, respectively. The behavior of $D_{\rm tot}$ is illustrated in Fig. 7, where we also fitted the functions according to Eqs. (15) and (16) in the damage and fragmented regimes, respectively. The best fits were obtained with the exponents 4.5 and 0.29, which agree very well with the above predictions. The high quality of the results presented in Fig. 7 demonstrates the consistency of our scaling analysis.

VI. DISCUSSION

We investigated the fragmentation of spherical solid bodies due to impact with a hard wall using a discrete element model of heterogeneous brittle materials in three dimensions. Depending on the impact velocity, the final outcome of the breakup process is classified as damage when most particles remain in one piece. Fragmentation occurs when a considerable size reduction is achieved (i.e., when the largest fragment becomes significantly smaller than the original size of the body). We focused on the damage-fragmentation transition which emerges at a well defined critical impact velocity.

Simulations were performed at four different system sizes varying the impact velocity within a broad range. To determine the critical exponents of the transition, we carried out a finite size scaling analysis of the simulated data. The critical point of the transition from the damage to the fragmentation phase of finite size systems was identified at the impact velocity where the average fragment mass takes a maximum value. Assuming the scaling structure characteristic for continuous phase transitions near a critical point, high quality data collapse was obtained for the mass of the largest fragment normalized by the total mass and for the average fragment mass. The scaling analysis proved the validity of the phase transition picture of impact fragmentation phenomena and yielded the critical exponents of the damage-fragmentation transition with a good accuracy.

The universality of the exponent of the fragment mass distribution is a crucial feature of fragmentation phenomena [2–6,9]. For impact-induced breakup a large amount of experiments on heterogeneous brittle materials confirmed that the exponent is independent of the imparted energy in the fragmented phase, however, it can vary according to the geometry (aspect ratio) of the sample since it affects the crack structure. Recent simulations of a generic model of fragmentation questioned the universality, predicting a logarithmic increase of the exponent with the imparted energy [13,14]. To resolve this problem, we carefully analyzed the scaling behavior of fragment mass distributions obtained at different impact velocities. Although single distributions might suggest a spurious increase of the exponent, the high quality data collapse obtained by rescaling the distributions with the average fragment mass reveals universality, at least in the range of impact velocities where the mass distribution is unimodal, comprising a power law with an exponential cutoff. Our analysis showed that, although DEM simulations can be very realistic, their serious limitation is the relatively small system size and the existence of unbreakable elementary units. It has the consequence that power laws span only over a limited range so that the apparent change of the mass distribution exponent may even be caused by the shifting cutoff of the distribution and by the unrealistic increase of the fraction of powder accumulating in the form of unbreakable single particles. For the accurate determination of the exponents of power law distributed fragment masses it is recommended first to scale the data and then to fit the scaling function together with its cutoff.

To characterize the time evolution of the breakup process, we analyzed the scaling behavior of damage rate functions dD/dt obtained at different impact velocities. Based on the scaling structure of dD/dt, we showed that the total amount of damage increases as a power law of the impact velocity in the damage phase, however, in the fragmented regime a power law is obtained as a function of the distance from the critical point. It is important to emphasize that this functional behavior is the consequence of the dimensionality of the system: In two dimensions DEM simulations provided a logarithmic dependence of the total damage with the impact velocity

[13,14,20]. Our analysis revealed that in three dimensions the evolution of damage is characterized by power laws due to the Hertz type contact of the spherical body with the hard plate.

In the damaged and fragmented regimes the characteristic time scale of the breakup process was found to decrease as a power law of the impact velocity and of the distance from the critical point, respectively. When the sample retains its integrity (damage) the scaling exponent falls close to the exponent characterizing the velocity dependence of the duration of Hertz contacts. However, when fragmentation is achieved the exponent becomes significantly smaller (i.e., its value is nearly half of the Hertz exponent [18,19]).

ACKNOWLEDGMENTS

The work is supported by TAMOP-4.2.1/B-09/1/KONV-2010-0007 project. The project is implemented through the New Hungary Development Plan, cofinanced by the European Social Fund and the European Regional Development Fund. F. Kun acknowledges the support of OTKA K84157. This work was supported by the European Commissions by the Complexity-NET pilot project LOCAT. The work is supported by the TAMOP-4.2.2/B-10/1-2010-0024 project. The project is cofinanced by the European Union and the European Social Fund. We thank KTI Project 13703.1 PFFLR-IW.

[1] J. A. Aström, Adv. Phys. **55**, 247 (2006).
[2] F. K. Wittel, F. Kun, H. J. Herrmann, and B. H. Kröplin, Phys. Rev. Lett. **93**, 035504 (2004).
[3] F. Kun, F. K. Wittel, H. J. Herrmann, B. H. Kröplin, and K. J. Maloy, Phys. Rev. Lett. **96**, 025504 (2006).
[4] J. A. Aström, F. Ouchterlony, R. P. Linna, and J. Timonen, Phys. Rev. Lett. **92**, 245506 (2004).
[5] J. A. Aström, R. P. Linna, J. Timonen, P. F. Möller, and L. Oddershede, Phys. Rev. E **70**, 026104 (2004).
[6] G. Timár, J. Blömer, F. Kun, and H. J. Herrmann, Phys. Rev. Lett. **104**, 095502 (2010).
[7] F. Kun and H. J. Herrmann, Comp. Meth. Appl. Mech. Eng. **138**, 3 (1996).
[8] G. A. D'Addetta, F. Kun, and E. Ramm, Granular Matter **4**, 77 (2002).
[9] F. Kun and H. J. Herrmann, Phys. Rev. E **59**, 2623 (1999).
[10] H. Katsuragi, D. Sugino, and H. Honjo, Phys. Rev. E **68**, 046105 (2003).
[11] H. Katsuragi, D. Sugino, and H. Honjo, Phys. Rev. E **70**, 065103(R) (2004).
[12] C. F. Moukarzel, S. F. Fernandez-Sabido, and J. C. Ruiz-Suarez, Phys. Rev. E **75**, 061127 (2007).
[13] N. Sator and H. Hietala, Int. J. Fract. **163**, 101 (2010).
[14] S. M. N. Sator and F. Sausset, Europhys. Lett. **81**, 44002 (2008).
[15] H. A. Carmona, F. K. Wittel, F. Kun, and H. J. Herrmann, Phys. Rev. E **77**, 051302 (2008).
[16] *Computer Simulation of Liquids*, edited by M. P. Allen and D. J. Tildesley, (Oxford University Press, Oxford, 1984).
[17] T. Pöschel and T. Schwager, *Computational Granular Dynamics* (Springer, Berlin, 2005).
[18] K. L. Johnson, *Contact Mechanics* (Cambridge University Press, New York, 1985).
[19] W. J. Stronge, *Impact Mechanics* (Cambridge University Press, New York, 2000).
[20] B. Behera, F. Kun, S. McNamara, and H. J. Herrmann, J. Phys.: Condens. Matter **17**, 2439 (2005).
[21] D. Stauffer and A. Aharony, *Introduction to Percolation Theory* (Taylor & Francis, London, 1992).
[22] H. Nishimori and G. Ortiz, *Elements of Phase Transitions and Critical Phenomena*, 1st ed., (Oxford University Press, Oxford, 2011).
[23] H. Katsuragi, H. Honjo, and S. Ihara, Phys. Rev. Lett. **95**, 095503 (2005).
[24] T. Kadono and M. Arakawa, Phys. Rev. E **65**, 035107 (2002).
[25] T. Kadono, Phys. Rev. Lett. **78**, 1444 (1997).
[26] F. P. M. dos Santos, V. C. Barbosa, R. Donangelo, and S. R. Souza, Phys. Rev. E **81**, 046108 (2010).
[27] A. Meibom and I. Balslev, Phys. Rev. Lett. **76**, 2492 (1996).
[28] E. Villermaux, Annu. Rev. Fluid Mech. **39**, 419 (2007).
[29] K. T. Chau, X. X. Wei, R. H. C. Wong, and T. X. Yu, Mech. Mater. **32**, 543 (2000).
[30] H. Inaoka, E. Toyosawa, and H. Takayasu, Phys. Rev. Lett. **78**, 3455 (1997).
[31] A. Diehl, H. A. Carmona, L. E. Araripe, J. S. Andrade, and G. A. Farias, Phys. Rev. E **62**, 4742 (2000).
[32] C. D. Lorenz and M. J. Stevens, Phys. Rev. E **68**, 021802 (2003).
[33] J. A. Aström, B. L. Holian, and J. Timonen, Phys. Rev. Lett. **84**, 3061 (2000).
[34] S. Steacy and C. Sammis, Nature (London) **353**, 250 (1991).
[35] A. Levandovsky and A. C. Balazs, Phys. Rev. E **75**, 056105 (2007).
[36] J. Åström and J. Timonen, Phys. Rev. Lett. **78**, 3677 (1997).
[37] P. Kekalainen, J. A. Aström, and J. Timonen, Phys. Rev. E **76**, 026112 (2007).
[38] K. J. Maloy, S. Santucci, J. Schmittbuhl, and R. Toussaint, Phys. Rev. Lett. **96**, 045501 (2006).
[39] K. T. Tallakstad, R. Toussaint, S. Santucci, J. Schmittbuhl, and K. J. Maloy, Phys. Rev. E **83**, 046108 (2011).
[40] L. Laurson, S. Santucci, and S. Zapperi, Phys. Rev. E **81**, 046116 (2010).